



# Glacial-interglacial transitions in microbiomes recorded in deep-sea sediments from the western equatorial Atlantic

Lucas Freitas<sup>a,b,1</sup>, Luciana Appolinario<sup>a,b,1</sup>, Gabriela Calegario<sup>a,b</sup>, Mariana Campeão<sup>a,b</sup>, Diogo Tschoeke<sup>a,b</sup>, Gizele Garcia<sup>a,b</sup>, Igor Martins Venancio<sup>c,d</sup>, Carlos A.N. Cosenza<sup>b</sup>, Luciana Leomil<sup>b</sup>, Marcelo Bernardes<sup>d</sup>, Ana Luiza Albuquerque<sup>d,\*</sup>, Cristiane Thompson<sup>a,b,\*\*</sup>, Fabiano Thompson<sup>a,b,\*\*</sup>

<sup>a</sup> Institute of Biology, Federal University of Rio de Janeiro (UFRJ), Rio de Janeiro, Brazil

<sup>b</sup> SAGE-COPPE, UFRJ, Rio de Janeiro, Brazil

<sup>c</sup> Center for Weather Forecasting and Climate Studies (CPTec), National Institute for Space Research (INPE), Cachoeira Paulista, Brazil

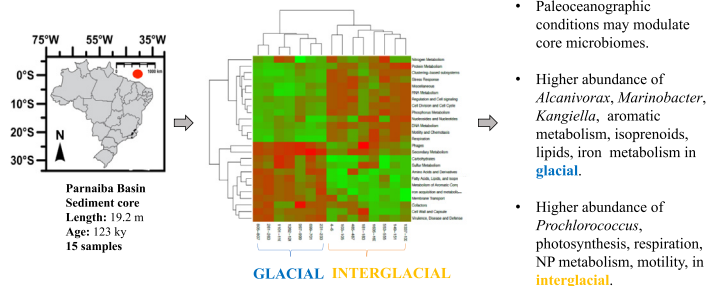
<sup>d</sup> Graduate Program on Geoscience (Geochemistry), Federal Fluminense University, Niterói, Brazil

## HIGHLIGHTS

- Paleoclimatographic conditions may modulate core microbiomes.
- *Alcanivorax*, *Marinobacter*, and *Kangiella* are abundant in glacial periods.
- *Prochlorococcus* are abundant in interglacial periods.
- Aromatics, isoprenoids, lipids, iron metabolisms are abundant in glacial.
- Photosynthesis, respiration, motility, NP metabolism, in interglacial

## GRAPHICAL ABSTRACT

### Paleoclimatic microbiome transitions



## ARTICLE INFO

### Article history:

Received 9 June 2020

Received in revised form 9 July 2020

Accepted 9 July 2020

Available online 19 July 2020

Editor: Frederic Coulon

### Keywords:

Metagenomics

Sediment core

Bioindicator

Amazon river

Microbiome modulation

## ABSTRACT

In the late Quaternary, glacial-interglacial transitions are marked by major environmental changes. Glacial periods in the western equatorial Atlantic (WEA) are characterized by high continental terrigenous input, which increases the proportion of terrestrial organic matter (e.g. lignin, alkanes), nutrients (e.g. iron and sulphur), and lower primary productivity. On the other hand, interglacials are characterized by lower continental contribution and maxima in primary productivity. Microbes can serve as biosensors of past conditions, but scarce information is available on deep-sea sediments in the WEA. The hypothesis put forward in this study is that past changes in climate conditions modulated the taxonomic/functional composition of microbes from deep sediment layers. To address this hypothesis, we collected samples from a marine sediment core located in the WEA, which covered the last 130 kyr. This region is influenced by the presence of the Amazon River plume, which outputs dissolved and particulate nutrients in vast oceanic regions, as well as the Parnaíba river plume. Core GL-1248 was analysed by shotgun metagenomics and geochemical analyses (alkane, lignin, perylene, sulphur). Two clusters (glacial and interglacial-deglacial) were found based on taxonomic and functional profiles of metagenomes. The interglacial period had a higher abundance of genes belonging to several sub-systems (e.g. DNA, RNA metabolism, cell division, chemotaxis, and respiration) that are consistent with a past environment with enhanced primary productivity. On the other hand, the abundance of *Alcanivorax*, *Marinobacter*, *Kangiella* and aromatic compounds that may serve as energy sources for these bacteria were higher in the glacial. The glacial period was enriched in

\* Corresponding author.

\*\* Corresponding authors at: Institute of Biology, Federal University of Rio de Janeiro (UFRJ), Rio de Janeiro, Brazil.

E-mail addresses: [ana\\_albuquerque@id.uff.br](mailto:ana_albuquerque@id.uff.br) (A.L. Albuquerque), [thompsoncristiane@gmail.com](mailto:thompsoncristiane@gmail.com) (C. Thompson), [fabianothompson1@gmail.com](mailto:fabianothompson1@gmail.com) (F. Thompson).

<sup>1</sup> the two authors contributed equally to this study.

genes for the metabolism of aromatic compounds, lipids, isoprenoids, iron, and Sulphur, consistent with enhanced fluvial input during the last glacial period. In contrast, interglacials have increased contents of more labile materials originating from phytoplankton (e.g. *Prochlorococcus*). This study provides new insights into the microbiome as climatic archives at geological timescales.

© 2020 Published by Elsevier B.V.

## 1. Introduction

Deep-sea sediments are important archives of oceanic changes at geological timescales. The evolution of oceanic conditions and changes in marine biodiversity during Earth's history are commonly obtained from microfossils (Kucera, 2007). However, the study of microfossils lacks fundamental information concerning the metabolic repertoire of microbiomes in past climatic conditions. Microbes can be biosensors of past conditions (Orsi et al., 2017), but scarce information is available on deep-sea sediment ecosystems (Danovaro et al., 2010; Danovaro et al., 2014; Kodzius and Gojobori, 2015).

The majority of previous studies concentrated on hydrothermal vents, cold sediments, and subsurface sediments (Corinaldesi, 2015; Mullineaux et al., 2018). Only a few studies have elucidated the microbial taxonomic and functional diversity of sediment cores from tropical regions. They suggested that microbes have a role in the remineralisation of organic matter, nutrient cycling, and energy flow to higher trophic levels (Kimes et al., 2013; Huang et al., 2019). Archaea are abundant in oxic and anoxic deep seafloor sediment layers in the North Atlantic Ocean (Vuillemin et al., 2019), but it is not known whether this pattern of dominance can be observed in similar environments, such as the Atlantic equatorial margin.

In the late Quaternary, glacial-interglacial transitions are marked by major changes in global temperature, CO<sub>2</sub>, size of ice sheets, relative sea level, humidity, and dust deposition, among others. Therefore, glacial-interglacial cycles are observed in several paleoclimate records globally. In the western equatorial Atlantic (WEA), glacial-interglacial changes have been reported in terrigenous input, organic matter source, and upper-ocean conditions (i.e. productivity and stratification) (Rühlemann et al., 1996; Jennerjahn et al., 2004; Venancio et al., 2018; Fadina et al., 2019). For the late Quaternary, glacial periods in the WEA are characterized by high continental terrigenous input due to the low relative sea level, which led to an increased proportion of terrestrial organic matter in the adjacent ocean and low primary productivity.

On the other hand, interglacials are characterized by less continental contribution and maxima in primary productivity. Thus, glacials are dominated by a more detritic and refractory organic material originating from enhanced fluvial input. In contrast, interglacials have higher contents of more labile materials originating from the primary production of marine phytoplankton (e.g., diatoms, picocyanobacteria). Records of total organic carbon (TOC) and iron intensities (Fe) from sediment core GL-1248 located in the WEA show enhanced fluvial input and terrestrial organic matter contribution (Fig. 1A) during glacials, which is also supported by other geochemical proxies (Fadina et al., 2019). We can also observe such patterns by comparing both proxies (TOC and Fe) between glacial and interglacial-deglacial samples from core GL-1248 (Fig. 1B–C), evidencing significant differences between these periods.

Metagenomics has been applied more recently to marine sediments to gain insights on the metabolic repertoire of microbiomes under past climatic conditions (Orsi et al., 2017; Biller et al., 2018). Microbiomes may reflect the paleoclimatic conditions at the taxonomic and functional levels, shedding light on fundamental processes occurring during glacial-interglacial cycles. The hypothesis put forward in this study is that past changes in climate conditions modulated the taxonomic and functional composition of microbes of deep sediment layers. To address this hypothesis, we collected samples from a marine sediment core (GL-1248) located in the WEA, which covers the last 130 kyr (Venancio et al.,

2018; Fadina et al., 2019). This region is influenced by the presence of the Amazon river plume, which outputs dissolved and particulate nutrients in vast oceanic regions (Moura et al., 2016; Francini-Filho et al., 2018), as well as the Parnaíba river plume, which is one of the most important fluvial systems of North-eastern Brazil.

Previous studies in this area have shown glacial-interglacial changes in continental terrigenous input, sources of organic matter, and upper-ocean conditions (Venancio et al., 2018; Fadina et al., 2019). However, there is scarce knowledge about the possible modulation of microbiomes by such glacial-interglacial transitions. Thus, the taxonomic and functional profiles of microbiomes for core GL-1248 were analysed. Metagenome-assembled genomes (MAGs) were obtained to characterize the dominant types of microbes across the entire sediment core. We also performed new geochemical analyses to better characterize changes in sources of organic matter.

## 2. Materials and methods

### 2.1. Sampling site, age-depth model, and chemical analyses

Sediment core GL-1248 (0°55.20S, 43°24.1 0 W, 2264-m water depth, 19.29 m long) was retrieved by Petrobras on the continental slope off North-eastern Brazil. Venancio et al. (2018) published a chronology for the core. Its age model was based on 12 AMS radiocarbon ages for the upper core depth of 6.30 m. Radiocarbon dating indicates an age of about  $44.0 \pm 0.7$  ka at this core depth. For the lower part of the core (6.30 to 16.66-m core depth;  $\approx 44$ –129 ka), the chronology was derived from the alignment of the Ti/Ca record of core GL-1248 to the ice d<sup>18</sup>O record of the North Greenland Ice Core Project (NGRIP) (Andersen et al., 2004; Wolff et al., 2010).

In total, 16 sediment strata were analysed for metagenomics, ranging from 4 to 1602 cm. For all assays in this work, each stratum was analysed individually. Alkane, perylene, and lignin content were also measured across the sediment core. Lignin content was analysed through a described previously alkaline CuO oxidation procedure (Bernardes et al., 2004). The yields of lignin-derived phenols ( $\chi$ 8) were considered as the sum of three distinct groups: vanillyl phenols (V - vanillin, acetovanillone, vanillic acid), syringyl phenols (S - syringaldehyde, acetosyringone, syringic acid), and cinnamyl phenols (C - p-coumaric acid, ferulic acid) (Hedges and Ertel, 1982). The ratio of p-hydroxyacetophenone (pBn) to P - phenol group (pBn/P) was used to distinguish marine from terrestrial sources.

The alkane composition was determined as described previously (Wakeham and Canuel, 1988). Alkanes were identified from n-C16 to n-C40, as well as the isoprenoids pristane and phytane. Analyte determination in F2 (PAH and perylene) was carried out on a gas chromatograph coupled to a mass spectrometer (GC 7890A-MSD 5975 HP-Agilent), which was fitted with a capillary column (model VF-17 ms; 30 m, 0.25 mm, 0.25  $\mu$ m) (U.S. Environmental Protection Agency, 1996; U.S. Environmental Protection Agency, 2014). A mixed primary solution with a concentration of 100 ng mL<sup>-1</sup> was made with the 16 targeted PAH compounds (naphthalene, acenaphthene, acenaphene, fluorene, phenanthrene, anthracene, fluoranthene, pyrene, benzo(a)anthracene, chrysene, benzo(b)fluoranthene, benzo(k)-fluoranthene, benzo(a)pyrene, indene(1,2,3-c,d)pyrene, dibenzo(a,h)anthracene, and benzo(ghi)perylene), as well as deuterated internal standards (naphthalene-d8, acenaftene-d10, phenanthrene-d10, chrysene-d12, and perylene-d12). Mass spectrum data were obtained using an

electron ionization source (EI) at 70 eV and in full scan mode in the  $m/z$  range of 50 to 350. The only analyte detected was perylene.

## 2.2. DNA extraction, library construction, and sequencing

DNA was extracted using a DNA power soil extraction kit (Qiagen), and its quality was checked using agarose gel electrophoresis. Libraries were prepared using a Nextera XT DNA Sample Preparation Kit (Illumina, San Diego, CA, USA) in accordance with the manufacturer's protocol. The libraries' quality was analysed using a 2100 Bioanalyzer and the High Sensitivity DNA Kit (Agilent, Santa Clara, CA, USA) and 7500 Real Time PCR system (Applied Biosystems, Foster City, CA, USA) to evaluate the size and accuracy of the quantification, respectively. Sequencing was performed using an Illumina MiSeq sequencer (600 cycles overlapping paired-end reads) (Illumina, San Diego, CA, USA).

## 2.3. Bioinformatic analysis

Low-quality sequenced regions and adaptors from Illumina raw reads were removed with PRINSEQ v. 0.20.4 (Schmieder and Edwards,

2011), and we used pear v. 0.9.11 (Zhang et al., 2014) to merge paired-end reads. Next, we characterize each metagenome based on their taxonomy and function using the MG-RAST pipeline (Meyer et al., 2018). For phylum, class, and genus taxonomic analyses, we only considered groups higher than 1%, 1%, and 0.4% at each depth, respectively. To characterize and identify new microbial species, we used all metagenomes to build metagenome-assembled genomes (MAGs) using metaSPAdes v. 3.10 (Nurk et al., 2017). The genome assembly starts with metagenomic binning, in which assembly DNA reads into contigs. These contigs are then binned into putative partial or complete MAGs (Bowers et al., 2017).

In the next step, we evaluated the MAGs' completeness and contamination using checkM (Parks et al., 2015) and we used GTDB-Tk (Chaumeil et al., 2019) to perform a taxonomic classification. MAGs were considered as new species if they had >45% completeness, <10% contamination, and <95% Average Nucleotide Identity (ANI) compared with any other genome in GTDB database (Parks et al., 2018). Following this assessment, we pruned the GTDB-Tk phylogenetic tree (containing approximately 23,000 species) to select the closest species from our MAGs using the ape package (Paradis et al., 2004) in the R language (R Core Team, 2019) and edited them with FigTree.

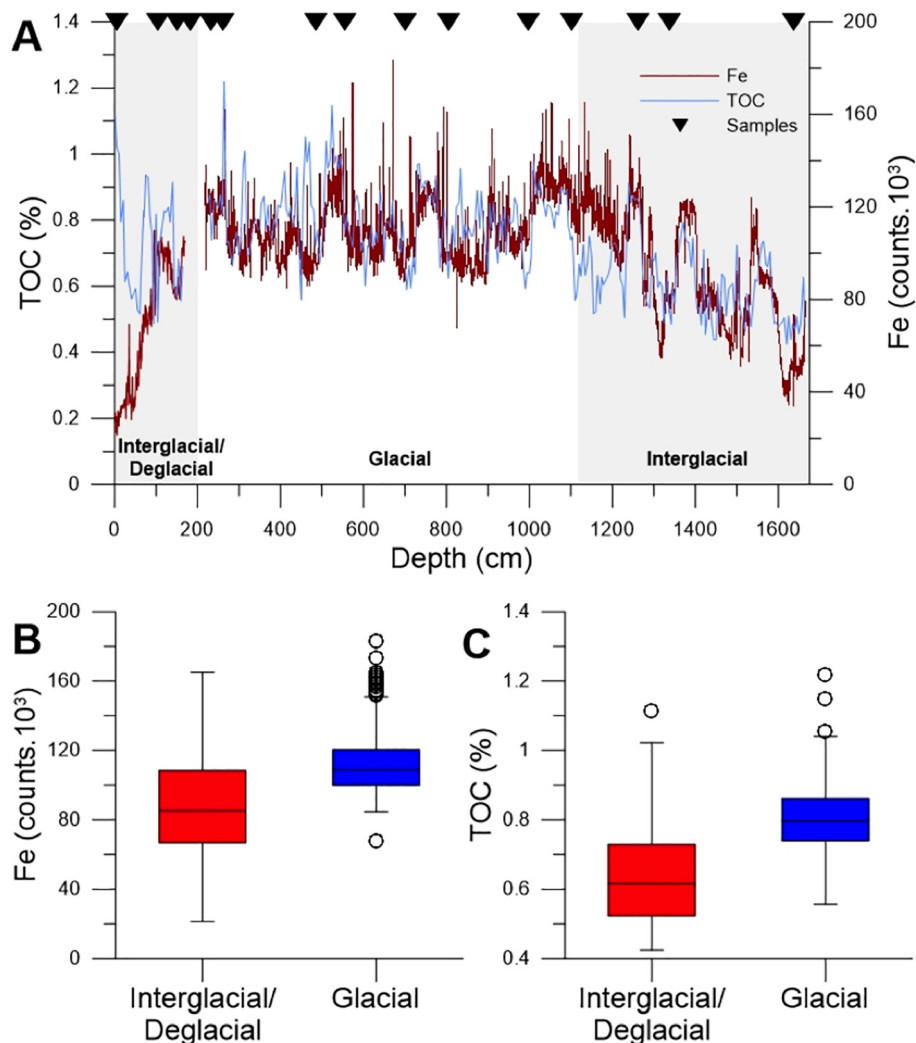


**Fig. 1.** Glacial-Interglacial differences in total organic carbon (TOC) and iron intensities (Fe) for core GL-1248, with the position of the samples collected for this study. (A) Total Organic Carbon (TOC, %) (blue line) and Iron (Fe, counts.10<sup>3</sup>) (red line) of core GL-1248 from Fadina et al. (2019). (B) Box-whisker plot of Fe (counts.10<sup>3</sup>) values from glacial (blue) and interglacial/deglacials (red) periods within core GL-1248. (C) Box-whisker plot of TOC (%) values from glacial (blue) and interglacial/deglacials (red) periods within core GL-1248. The open circles represent the outliers. A two-sample *t*-test (see supplementary material) show that TOC and Fe mean for glacial and interglacials are statistically different ( $p$ -value<<0.01). The black triangles in panel (A) mark the position of the collected samples for metagenomic analyses. The grey bars mark the interglacials (i.e., MIS 5a-e and MIS 1), as well as the deglacial periods. (For interpretation of the references to color in this figure legend, the reader is referred to the web version of this article.)

**Table 1**  
Geochemical results for core GL-1248. Total organic carbon (TOC), carbon:nitrogen molar ratios (C:N), organic matter-carbon and nitrogen stable isotopes ( $\delta^{13}\text{C}$  and  $\delta^{15}\text{N}$ ), lignin, pBn/P ratio and perylene. For classification purposes, the entire MIS 5 was considered as an interglacial. Sample 181–183 cm is marked due to the high uncertainty of its age, but it within the last glacial-deglacial transition. (n.a – not available).

Depth (cm)	Age (kyr)	Period	TOC (%)	$\delta^{13}\text{C}$ (‰)	$\delta^{15}\text{N}$ (‰)	C:N	Fe (counts)	S (counts)	Lignin (mg.100mgOC <sup>-1</sup> )	pBn/P	Alkanes ( $\mu\text{g.g}^{-1}$ )	Perylene (ng.g <sup>-1</sup> )
4–6	1.42	Interglacial	1.02	-19.17	6.42	6.30	29,465	1842	0.08	0.37	5.99	0.0
103–105	11.52	Interglacial	0.49	-22.82	5.13	4.50	102,293	1306	0.18	0.35	18.33	60.1
149–151	13.73	Deglacial	0.57	-21.81	6.25	5.33	82,897	1586	0.21	0.49	9.23	16.0
181–183	14.8–29.1	Deglacial*	0.73	22.09	4.53	6.10	115,001	1571	n.a	n.a.	n.a	n.a
231–233	29.24	Glacial	0.88	-22.12	4.48	7.03	121,286	2054	0.23	0.35	3.69	18.5
261–263	29.69	Glacial	0.82	-20.63	4.62	6.81	117,758	2095	0.22	0.23	15.64	37.3
485–487	37.42	Glacial	0.72	-22.60	6.52	7.22	99,538	2347	0.20	0.16	12.51	107.4
553–555	39.47	Glacial	0.75	-20.73	5.99	8.16	128,841	6403	0.23	0.35	23.30	28.0
699–701	46.04	Glacial	0.70	-21.94	6.25	7.15	88,510	2043	0.40	0.09	5.16	80.8
805–807	49.94	Glacial	0.62	-21.18	5.61	7.67	96,910	2123	0.21	0.15	7.82	118.6
997–999	58.94	Glacial	0.64	-22.84	5.95	7.27	106,049	1425	0.14	0.54	n.a	38.5
1101–1103	70.45	Glacial	0.74	-21.57	5.57	7.88	126,597	2040	0.30	0.13	2.75	10.1
1262–1264	78.14	Interglacial	0.85	-23.38	5.90	8.31	130,197	2334	0.42	0.17	12.11	57.2
1337–1339	83.50	Interglacial	0.55	-21.00	6.78	6.01	76,993	1327	0.19	0.25	3.75	41.3
1519–1521	106.42	Interglacial	0.46	-21.54	6.56	6.10	80,919	1196	0.15	0.36	31.47	19.9
1635–1637	123.31	Interglacial	0.49	-21.35	6.96	5.80	47,678	1075	0.09	0.53	n.a	18.1

After MAG construction, we assembled a custom database of oil-degradation genes composed of BTEX, PAH, Phenol, and Alkane and used it to search for these genes in each MAG. Lastly, we used R v. 3 (R Core Team, 2019) to conduct a Canonical Component Analysis (CCA) and heatmap analysis. To draw all graphics, the following R packages were used: tidyverse v. 1.3 (Wickham et al., 2019), reshape2 v. 1.4.4 (Wickham, 2007), and RColorBrewer v. 1.1-2 (Harrover and Brewer, 2003).

### 3. Results and discussion

#### 3.1. Geochemical analyses

A higher concentration of lignin (0.24 mg · 100 mg OC<sup>-1</sup>) and lower values of the pBn/P ratio (0.25) were observed during the glacial period (Table 1), while the opposite trend was observed for interglacial and deglacial periods (0.16 and 0.36 mg · 100 OC<sup>-1</sup>, respectively) (Fig. 2).

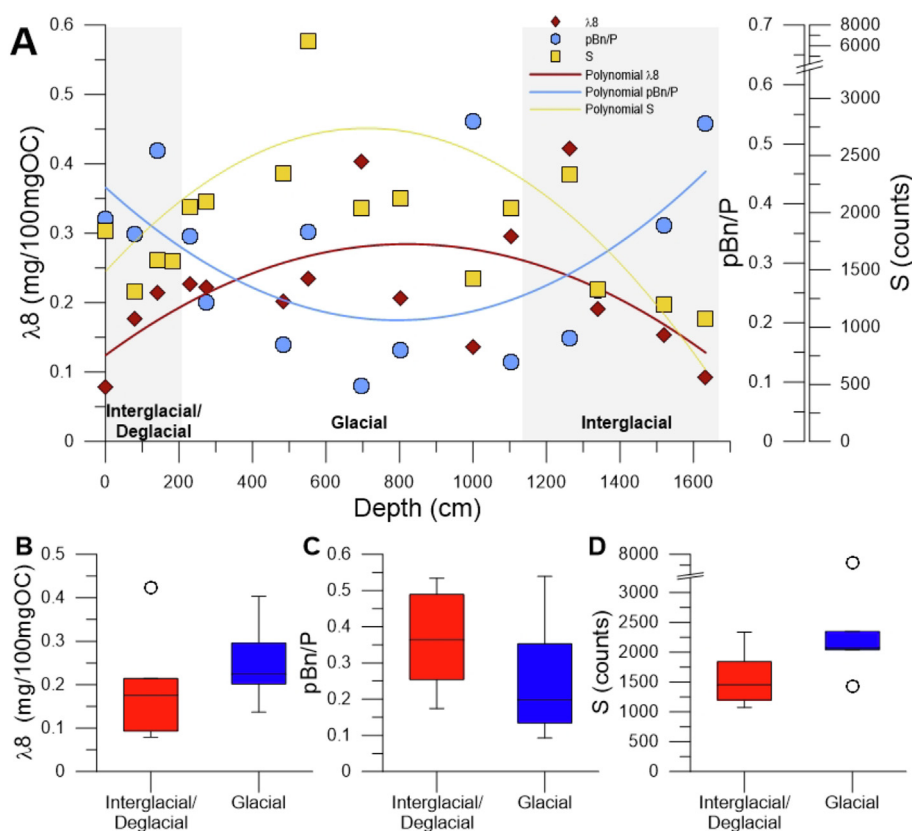


**Fig. 2.** Glacial-interglacial differences in lignin and pBn/P for core GL-1248. (A) pBn/P ratio (blue circles), lignin  $\lambda_8$ , mg.100mgOC<sup>-1</sup> (red diamonds) and sulphur (yellow squares) of core GL-1248, with their respective polynomial fits. (B) Box-whisker plot of lignin values from glacial (blue) and interglacial/deglacials (red) periods within core GL-1248. (C) Box-whisker plot of pBn/P values from glacial (blue) and interglacial/deglacials (red) periods within core GL-1248. The open circles represent the outliers. The grey bars mark the interglacials (i.e., MIS 5a-e and MIS 1), as well as the deglacial periods. (For interpretation of the references to color in this figure legend, the reader is referred to the web version of this article.)

**Table 2**  
Sequencing and domain statistics for all samples.

Sample (cm)	Size (nt)	# reads	Length (nt)	GC (%)	Bacteria (%)	Archaea (%)	Eukaryota (%)	Viruses (%)
4–6	76,326,482	310,603	246 ± 84	51 ± 11	96.07	2.82	1.01	0.10
103–105	126,504,836	582,009	217 ± 71	54 ± 10	98.90	0.56	0.51	0.03
181–183	281,957,486	1,091,675	258 ± 86	58 ± 10	99.40	0.30	0.28	0.02
231–233	282,469,213	1,213,891	233 ± 74	59 ± 10	99.40	0.30	0.28	0.02
261–263	268,672,769	1,137,849	236 ± 80	60 ± 10	99.36	0.34	0.27	0.02
485–487	286,382,053	1,127,673	254 ± 81	56 ± 11	99.22	0.39	0.36	0.02
491–151	230,527,916	959,257	240 ± 80	54 ± 10	99.21	0.42	0.35	0.01
553–55	251,817,526	962,482	262 ± 89	51 ± 11	98.78	0.50	0.69	0.02
699–701	315,878,453	1,223,647	258 ± 85	60 ± 10	99.51	0.21	0.26	0.03
805–807	291,134,895	1,159,111	251 ± 85	61 ± 10	99.50	0.26	0.23	0.02
997–999	67,361,315	282,236	239 ± 75	59 ± 11	99.44	0.26	0.28	0.02
1101–1103	257,137,233	1,007,509	255 ± 83	56 ± 11	99.46	0.22	0.27	0.06
1262–1264	244,852,563	980,519	250 ± 86	58 ± 11	99.58	0.18	0.18	0.06
1337–1339	150,064,896	613,592	245 ± 91	54 ± 12	99.31	0.39	0.30	0.01
1635–1637	136,893,514	559,658	245 ± 90	54 ± 10	99.42	0.17	0.38	0.02

Higher values of sulphur were observed in the glacial (Fig. 2; Table 1). Total alkanes varied from  $2.75 \mu\text{g}\cdot\text{g}^{-1}$  in the range of 1101–1103 cm (70.45 kyr) to  $31.47 \mu\text{g}\cdot\text{g}^{-1}$  in the range of 1519–1521 cm (106.42 kyr) (Table 1). The mean value of total alkane for the glacial ( $10.12 \pm 7.47 \mu\text{g}\cdot\text{g}^{-1}$ ) and interglacial ( $13.48 \pm 10.17 \mu\text{g}\cdot\text{g}^{-1}$ ) were similar ( $p = .25$ ).

Unresolved complex mixture (UCM) is indicative of incomplete biodegraded hydrocarbon and was present in only the most recent sample (4–6 cm, 1.42 ka) with carbon maximum at n-C26 ( $23.5 \mu\text{g}\cdot\text{g}^{-1}$ ). Perylene was slightly higher in the glacial ( $54.9 \pm 41.6$ ) than in the interglacial ( $30.7 \pm 22.7$ ;  $p = .18$ ). Values of TOC, C:N,  $\text{d}^{13}\text{C}$ , and  $\text{d}^{15}\text{N}$  from Fadina et al. (2019) are shown for each of our samples (Table 1). TOC ranged between 1.02% (4–6 cm, 1.42 kyr) and 0.46% (1519–1521 cm, 106.42 kyr), but it did not follow any directional tendency according to depth, like the C:N ratio. The minimum ratio (4.5) was measured at 103–105 cm (11.52 kyr), and the highest value (8.31) was measured at 1264–1265 cm (78.14 kyr) (Table 1). Most of the high C:N values were observed during the glacial period. Stable carbon and nitrogen isotopes showed slight but consistent changes between interglacial-deglacial samples ( $-21.38\%$  and  $6.09\%$ , respectively) and glacial 8samples ( $-21.90\%$  and  $5.65\%$ , respectively), which support the increase in more refractory terrigenous organic matter during the glacial period.

### 3.2. Taxonomic features of metagenomes

The metagenomes were composed of 99.1% bacterial sequences and 0.49% archaeal sequences (Table 2). Totals of 62 phyla, 146 classes, 275 orders, 473 families, and 928 genera were found across all 15 core strata metagenomes (Fig. 3A–C). The most heterogeneous depth was at the surface (4–6 cm), comprising at least 23 abundant bacterial and archaeal classes (Fig. 3B), but diversity diminished across depth. This surficial sediment (4–6 cm) was also the most heterogeneous and clustered apart from other interglacial samples (Fig. 4A). The surface samples (4–6 cm) is the youngest, and thus, reflects the shortest timespan within the interglacial. Depths of 231–233 cm (29.24 kyr) and 805–807 cm (49.94 kyr) were similar (Fig. 4A, B) and these sediment depths are typical of glacials. The obtained grouping reinforces our hypothesis that metagenomes may be used to reveal paleoclimatic signals.

The dominant phylum in Archaea was *Euryarchaota* (>74% abundance at all but two depths: 4–6 cm and 1337–1339 cm). The dominant Archaea classes were Methanomicrobia, ranging between 11.9% (4–6 cm) and 46.2% (1635–1637 cm), and Thermoprotei, which ranged from 6.7% (4–6 cm) to 18% (805–807 cm). Previous studies also reported an abundance of Archaea in sediment cores related to reduced

availability of organic matter and/or their metanotrophic metabolism (Danovaro et al., 2014).

The majority of the bacterial sequences corresponded to *Proteobacteria*, with values ranging from 61.81% (4–6 cm) to 92.74% (1101–1103 cm), followed by *Bacteroidetes*, ranging from 2.43% (1101–1103 cm) to 18.1% (4–6 cm) (Fig. 3A). The most abundant *Gammaproteobacteria* genera were *Kangiella* (1.2% to 30.6%; 4–6 to 1635–1637 cm), *Thioalkalivibrio* (1.34% to 26.76%; 149–151 to 261–263 cm), *Pseudomonas* (4.67% to 9.93%; 1635–1637 to 4–6 cm), *Marinobacter* (5.13% to 39.47%; 1262–1264 to 103–105 cm), *Nitrosococcus* (1.27% to 7.52%; 1635–1637 cm to 261–263 cm), and *Alcanivorax* (2.37% to 20.84%; 1337–1339 to 181–183 cm) (Fig. 3C).

The high abundance of *Gammaproteobacteria* may be related to the metabolic versatility of these bacteria. *Thioalkalivibrio* comprises chemolithoautotrophic sulphur-oxidizing bacteria that inhabit extreme environments, like soda lakes (Ahn et al., 2017). *Nitrosococcus* are chemolithoautotrophic and known to oxidize ammonia (Campbell et al., 2011), while *Alcanivorax* use aliphatic hydrocarbons (alkanes, lignin) in their metabolism, leading to hydrocarbon degradation (Naether et al., 2013). The abundance of certain genera (e.g. SRB and methanogens) increased with depth, while the abundance of other genera (e.g. fermenters) was relatively stable across the entire core, which is consistent with previous studies that suggest fermenters are paleoclimatic indicators (Orsi et al., 2017).

### 3.3. Glacial-interglacial modulation of microbiome taxonomy and function

Two major clusters were found based on taxonomic and functional profiles (Fig. 4). Based on genera composition, all the samples from the glacial period were grouped, except for samples from the strata of 699–700 cm and 997–998 cm, which were grouped within the interglacial cluster (Fig. 4A). *Alcanivorax*, *Kangiella*, and *Marinobacter* were more abundant during the glacial period (Fig. 4A). These bacteria degrade hydrocarbons (e.g. alkanes) as an energy source. This is consistent with the homogenous values of alkanes across the entire core. On the other hand, these genera had low abundance in hallmark samples of the interglacial (103–105 cm, 149–150 cm, 1337–1338 cm, and 1635–1636 cm).

A similar glacial-interglacial grouping pattern was also observed for functional information (Fig. 4B). However, different glacial strata (485–487 cm and 553–555 cm) were grouped with interglacial samples. Metagenomes corresponding to the glacial period covered the samples between 231 and 233 and 1262–1264 cm (29.24 to 78.14 ka) were enriched in genes of metabolism of secondary compounds, aromatic compounds, fatty acids, lipids, isoprenoids, iron, and sulphur (Fig. 4B). The increase of these genes is consistent with enhanced fluvial

input during the last glacial period at this site. Glacials at this site are characterized by enhanced fluvial input due to the low sea level, providing more refractory terrigenous organic matter to the deep ocean

(Venancio et al., 2018; Fadina et al., 2019). This is consistent with the high lignin values found in the glacial, which could be used by bacteria as an energy source.

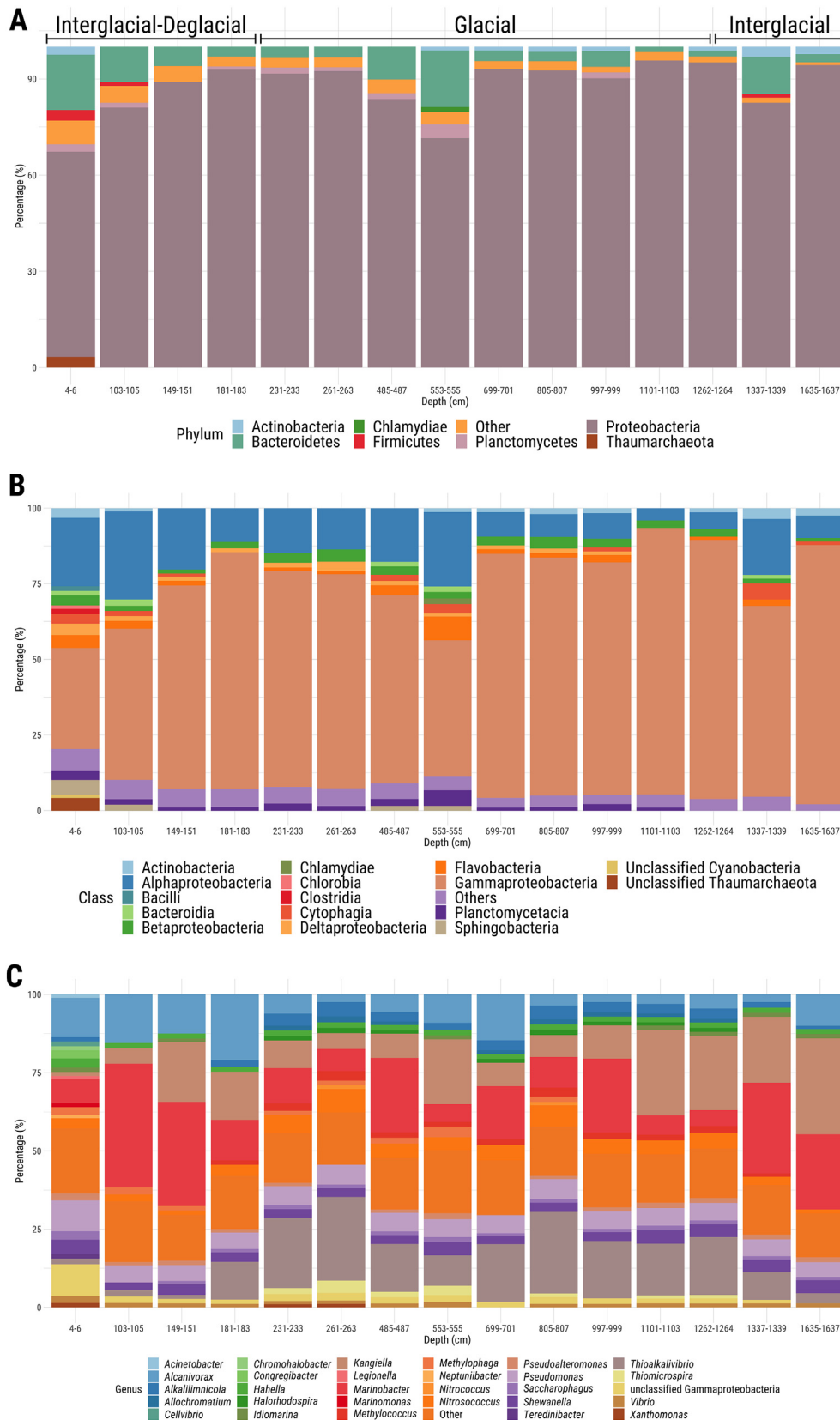


**Fig. 3.** Relative abundance from different Bacterial A) phyla, B) classes, and C) genus found along the core (4–1637 cm depth). The most abundant *Proteobacteria* classes were *Gamma*-, ranging from 29.67% (4–6 cm) to 76.31% (1101–1103 cm), followed by *Alpha*-, ranging from 5.51% (1101–1103 cm) to 28.21% (103–105 cm) (panel B).

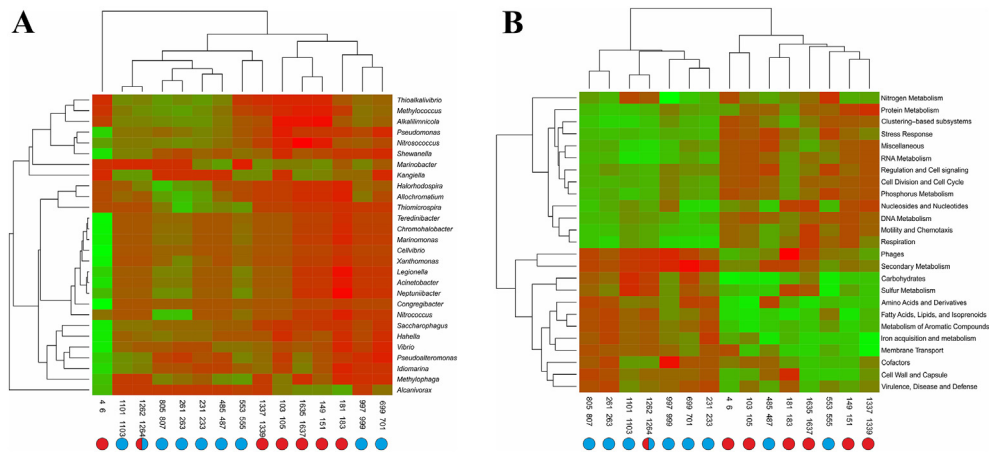


**Fig. 4.** Heatmap performed using the taxonomic and functional annotation according depth. Blue circles represent glacial periods and red circles represent interglacial periods. A) Taxonomic annotation using MG-RAST. B) The plot split metagenomics functions between two groups linked with depth (cm). Functional groups were obtained using MG-RAST (Seed, Level 1). (For interpretation of the references to color in this figure legend, the reader is referred to the web version of this article.)

Microbial degradation of lignin in soils reduces the original lignin content from  $>6$  mg/100 mg OC to the range of 1 to 4 mg/100 mg OC (Hedges et al., 1997). In the gradient from the coastal shelf to the deep ocean,  $\delta^{13}C$  drops to less than 1 mg/100 mg OC (Tesi et al., 2007). Oscillations in this range could be attributed to higher terrigenous input in the glacial period (Figs. 1 and 2). In addition, long-chain alkanes with odd carbon number distributions found in this study resemble those of n-alkanes from leaf waxes of higher plants (Eglinton and Hamilton, 1967) and in eolian dust samples (Simoneit et al., 1977), which supports a terrigenous origin of hydrocarbons.

The low alkane values found in some glacial samples (231–233 cm, 1101–1103 cm) had a prevalence of odd carbon number chains that are typical of vascular plants and could also be indicators of a terrigenous source. On the other hand, during interglacials, the sea level is higher than in glacials, so less material is transported from the land to the ocean, and less turbidity occurs in the water column. Non-lignin compounds relative to TOC contents may reflect contrasts in the contributions from soil/ancient sources that are poor in organic matter and fresh/rich plankton sources, as indicated by higher pBn/P ratios in the interglacial period (Fig. 2).

The source of perylene found across the entire sediment core may be due to formation in sediments in situ (Silliman et al., 1998). Higher amounts of perylene are not encountered until anoxic, deeper sediments are reached, suggesting that perylene formation requires precursor deposition under anoxic conditions (Garrigues et al., 1988). During the glacial period, higher concentrations of perylene were related to greater availability of refractory organic matter and lignin except for samples from 551 to 553 cm and in 1101–1103 cm, in which lower perylene values could be related the increase of odd alkanes. This indicates perylene degradation and more oxidized organic matter.

The higher abundance of iron, sulphur, and mercury metabolism found in the glacial period is consistent with high Fe and Hg concentrations found previously in the same period for core GL-1248 by Fadina et al. (2019). They argue that high atmospheric dust load during glacials increased the deposition of Fe + Hg complexes in the Parnaíba Basin, which were subsequently transported to the ocean. Despite being representative of glacial conditions, strata from 485 to 487 cm and 553–555 cm presented functional groups similar to those observed in interglacial samples. These probably reflect environmental variability during the glacial period, which is well-established for this region.

The clusters corresponding to the interglacial period are consistent with the paleoclimatic changes that cover Marine Isotopic Stages (MIS) 1 and 5, including the end of MIS 2, which is considered

as deglacial. This is represented by samples located at depths above 183 cm and below 1336 cm. In addition, as mentioned previously, two samples (486 and 554 cm) representative of the glacial were also grouped with the interglacial group, indicating great similarity between the microbial assemblages. This glacial inclusion reflects the natural variability during the glacial phase, which is marked by lower pulses of continental organic matter delivery (Fadina et al., 2019). In addition, it is worth mentioning that the stratum from 1262 to 1264 cm represents a condition of transition between an interglacial and glacial.

The interglacial period had a higher abundance of genes belonging to several sub-systems (e.g. membrane transport, protein/NDNA/RNA metabolism, cell division, motility, chemotaxis, and respiration), which are consistent with a past environment with enhanced primary

**Table 3**  
Major features of metagenome assembled genomes (MAGs).

Genome	ANI (%)	Closest phylogenetic neighbor	Completeness (%)	Contamination (%)	GC (%)
Genome.22	99.71	<i>Hydrogenovibrio crunogenus</i>	82.6	3.29	46
Genome.3	99.28	<i>Marinobacter</i> sp. 002744715	99.5	0.08	60
Genome.18	98.09	<i>Alcanivorax</i> sp. 002354605	98.09	0.32	65
Genome.30	97.21	<i>Arenibacter algicola</i>	97.21	1.88	42
Genome.8	94.53	<i>Kangiella</i>	79.6	6.28	45
Genome.5	90.12	<i>Alcanivorax</i>	95	2.6	59
Genome.10	88.28	<i>Marinobacter</i>	57.7	0	59
Genome.2	84.23	<i>Kangiella</i>	100	2.46	44
Genome.23	83.91	<i>Sunxiuqinia</i>	67.9	4.83	44
Genome.11	81.69	<i>Cyclobacterium</i>	100	0	42
Genome.4	79.46	<i>Gracilimonas</i>	99.7	0.56	41
Genome.16	78.18	<i>Methylophaga</i>	91.2	2.01	51
Genome.26	78.89	Rhodobacteraceae (f)	45.4	6.89	
Genome.13	N/A	Crocinitomicaceae (f)	100	0.54	38
Genome.14	N/A	Planctomycetaceae (f)	98.8	2.24	54
Genome.6	N/A	Rhodobacteraceae (f)	98.8	1.49	63
Genome.1	N/A	Ectothiorhodospirales (o)	98.5	0.91	66
Genome.15	N/A	Thiohalomonadales (o)	93.5	3.84	56
Genome.24	N/A	Thiohalomonadales (o)	67.3	1.05	49
Genome.27	N/A	Pseudomonadales (o)	66.7	4.67	

*Italic* = genus, (f) = family, (o) = order. N/A, GTDB provides no ANI match for the respective MAG as a possible result of high phylogenetic divergence.

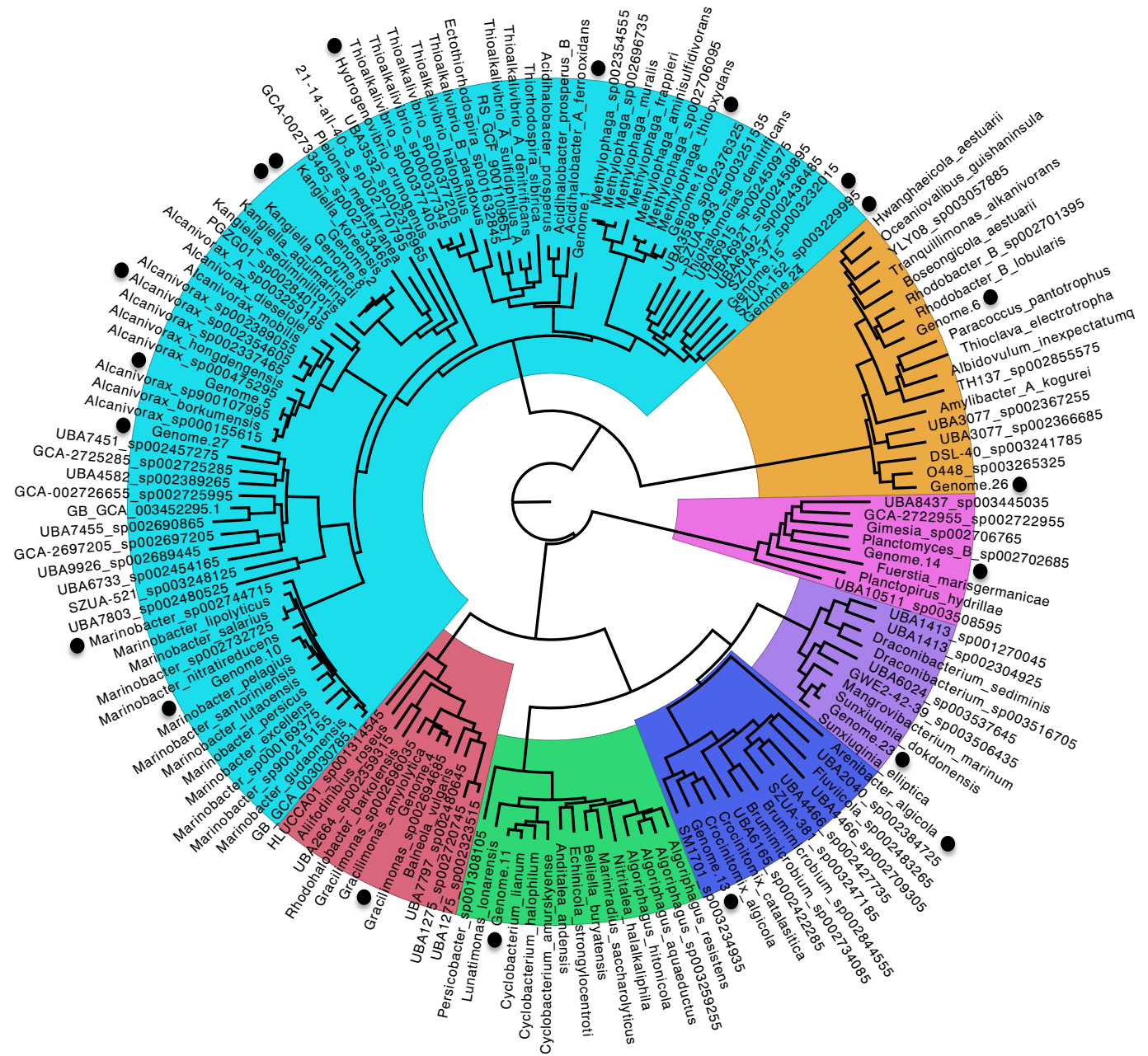


**Fig. 5.** Phylogenetic tree containing all 20 new MAGs. Each color represents a distinct class. The 20 new MAGs were distributed in seven classes. The most abundant class was *Gammaproteobacteria* (11 new MAGs). *Alphaproteobacteria* had two new MAGs and all other classes had one new MAG each.

productivity and microbial activity. In addition, the abundance of metagenomic sequences affiliated with the picoplanktonic primary producer *Prochlorococcus* was higher in the interglacial ( $p = .0079$ , glacial = 0.039%, interglacial = 0.067%). Meanwhile, *Synechococcus* was more abundant in the glacial period as a possible response to colder temperatures ( $p = .0017$ , glacial = 0.291%, interglacial = 0.197%). It was suggested that warm substages and interglacials in WEA are characterized by maxima in primary productivity, in contrast to glacial and cold substages (Rühlemann et al., 1996).

#### 3.4. Insights on novel bacterial species of deep-sea sediments from the WEA

All the twenty MAGs (except Genome.22 and Genome.30) belong to new species (Table 3; Fig. 5), with the majority belonging to new genera and families according to the GTDB-Tk toolkit (Table 3) (Parks et al.,

2020). Four genomes were classified at the known order level (*Ectothiorhodospirales*, *Thiohalomonadales*, and *Pseudomonadales*), while four genomes fell into known families, and eight genomes fell into known genera (Table 3). The novel genomes fell close to lipid, isoprenoid, and hydrocarbon-degrading bacteria.

*Oceanospirillaceae* genomes have a full cyclohexane degradation pathway, allowing them to react better in the presence of hydrocarbons in the environment (Dubinsky et al., 2013). Similarly, *Alcanivorax* genomes are typically hydrocarbonoclastic (Yakimov et al., 2019). The new genomes contain genes that enable them to degrade alkanes, such as cytochrome P450s, distinct alkane monooxygenases, AlkB homologous benzene, and toluene (Wang and Shao, 2013), as well as a monooxygenase related to the degradation of long-chain alkanes (Throne-Holst et al., 2007; Zadjelovic et al., 2020b). *Sunxiuqinia* and *Cyclobacterium* may metabolize aromatic compounds (Lim et al., 2016;

Shin and Kahng, 2017). Two new MAGs were classified into the genus *Kangiella* (*Gammaproteobacteria*, *Oceanospirillales*), which was previously found in the deep sea (*K. profundus*). *Oceanospirillales* are typical heterotrophs that use lipids and hydrocarbons in their metabolism (Appolinario et al., 2019; Appolinario et al., 2020).

To further elucidate the heterotrophic metabolic potential of the new MAGs, we searched for genes related to lipid, aromatic compound, and hydrocarbon degradation (BTEX, alkane, and naphthalene degradation). Genes found in the new MAGs belong to BTEX (49 genes), phenol (7 genes), PAH-alkane (6 genes), alkane (5 genes), and PAH (2 genes) (Supplementary Table 1). Levels of alkane and perylene found across the studied core are consistent with the presence of hydrocarbon degraders. Oil compounds found in the marine sediment tend to remain in anaerobic conditions, but many aromatic hydrocarbons, including BTEX, are known to be degraded even in anaerobic conditions. The presence of BTEX genes may be related to heterotrophic activity across the entire sediment core, supporting the notion that the novel microbes are metabolically versatile.

The present results are consistent with the previous hypothesis of a pool of indicator microbes existing across the deep sediment layers (Orsi et al., 2017). We confirmed this hypothesis that certain bacterial groups are enhanced in certain paleoclimatic conditions (e.g. *Alcanivorax*, *Kangiella*, *Marinobacter*, and *Pseudomonas*). These genera were more abundant during the glacial as a possible result of increased levels of hydrocarbons (e.g. alkanes) during this period. *Marinobacter* oxidizes different types of lipids (glycerolipids, branched, fatty acyls, and aromatic hydrocarbons) (Bonin et al., 2015). *Marinobacter* and other microbes are capable of using lipids and fatty acids as a sole source of energy in aerobic conditions (Bonin et al., 2015; Campeão et al., 2017; Appolinario et al., 2019) as a possible response to vast amounts of hydrocarbons (e.g. alkanes) produced by dominant marine picoplanktonic cyanobacteria *Synechococcus* and *Prochlorococcus* in the global ocean (Lea-Smith et al., 2015), suggesting certain metabolic interdependence of these microbial guilds. Similarly, *Alcanivorax* hydrolyses natural and synthetic polyesters (polyhydroxybutyrate, polyethylene, PBS) (Zadjelovic et al., 2020a), while several bacteria (e.g. *Pseudomonas*, *Rhodobacteraceae*) present in deep sediment layers and seawater can produce these polyesters as intracellular storage material and possible nutrient sources. These findings are consistent with the microbial abundance found in the present study. The novelty found among MAGs corroborates the hypothesis that metagenomes may be used to reveal paleoclimatic signals in deep sediment layers. Past changes in climate conditions can modulate the taxonomic and functional diversity of microbes, with the occurrence of several new taxa (including family rank) in deep sediment layers.

#### 4. Concluding remarks

This study has hinted at the possible modulation of deep-sea sediment microbiomes by glacial-interglacial environmental changes in the Brazilian equatorial margin. The different regional oceanic conditions regarding ocean primary productivity and fluvial input periods can act as drivers of taxonomic and functional diversity. Increase of relevant metabolic properties, such as respiration, cell division, RNA, DNA, and protein metabolism, are consistent with increased ocean productivity found in interglacial periods. Meanwhile, increases in secondary metabolites, lipids, fatty acids, isoprenoids, aromatic compounds, and iron acquisition are consistent with glacial periods.

The results of this study also demonstrate that deep sediment cores are sources of novel indicator genomes of past climatic conditions, such as those related to *Alcanivorax*, *Marinobacter*, and *Kangiella* in the glacial period. The abundance of these genomes in this period is consistent with a high concentration of aromatic compounds. These novel genomes are highly versatile metabolically, suggesting a possible pool of (in)organic nutrients in past (an)oxic environments.

Supplementary data to this article can be found online at <https://doi.org/10.1016/j.scitotenv.2020.140904>.

#### CRedit authorship contribution statement

**Lucas Freitas:** Methodology, Validation, Investigation, Formal analysis, Data curation, Writing - original draft, Writing - review & editing, Visualization. **Luciana Appolinario:** Methodology, Visualization. **Gabriela Calegario:** Methodology, Visualization. **Mariana Campeão:** Methodology, Formal analysis, Visualization. **Diogo Tschoeke:** Methodology, Formal analysis, Visualization. **Gizele Garcia:** Resources, Visualization. **Igor Martins Venancio:** Methodology, Visualization, Writing - review & editing. **Carlos A.N. Cosenza:** Methodology, Writing. **Luciana Leomil:** Methodology, Writing. **Marcelo Bernardes:** Formal analysis, Methodology. **Ana Luiza Albuquerque:** Resources, Writing - review & editing. **Cristiane Thompson:** Writing - review & editing, Visualization. **Fabiano Thompson:** Conceptualization, Validation, Resources, Writing - review & editing, Supervision, Project administration, Funding acquisition.

#### Declaration of competing interest

The authors declare that they have no known competing financial interests or personal relationships that could have appeared to influence the work reported in this paper.

#### Acknowledgments

The authors thank CNPq, CAPES, and FAPERJ.

#### References

- Ahn, A.-C., Meier-Kolthoff, J.P., Overmars, L., Richter, M., Woyke, T., Sorokin, D.Y., Muyzer, G., 2017. Genomic diversity within the haloalkaliphilic genus *Thioalkalivibrio*. *PLOS ONE* <https://doi.org/10.1371/journal.pone.0173517>.
- Andersen, K.K., Azuma, N., Barnola, J.M., Bigler, M., Biscaye, P., Caillon, N., Chappellaz, J., Clausen, H.B., Dahl-Jensen, D., Fischer, H., et al., 2004. High-resolution record of northern hemisphere climate extending into the last interglacial period. *Nature* 431, 147–151.
- Appolinario, L.R., Tschoeke, D., Paixão, R.V.S., Venas, T., Calegario, G., Leomil, L., Silva, B.S., Thompson, C.C., Thompson, F.L., 2019. Metagenomics sheds light on the metabolic repertoire of oil-biodegrading microbes of the South Atlantic Ocean. *Environ. Pollut.* 249, 295–304.
- Appolinario, L.R., Tschoeke, D., Calegario, G., Barbosa, L.H., Moreira, M.A., Albuquerque, A.L.S., Thompson, C.C., Thompson, F.L., 2020. Oil leakage induces changes in deep-sea sediments of Campos Basin (Brazil). *Sci. Total Environ.* 740, 139556.
- Bernardes, M.C., Martinelli, L.A., Krusche, A.V., Gudeman, J., Moreira, M., Victoria, R.L., Ometto, J.P.H.B., Ballester, M.V.R., Aufdenkampe, A.K., Richey, J.E., et al., 2004. Riverine organic matter composition as a function of land use changes, southwest Amazon. *Ecol. Appl.* 14.
- Billar, S.J., Berube, P.M., Dooley, K., Williams, M., Satinsky, B.M., Hackl, T., Hogle, S.L., Coe, A., Bergauer, K., Bouman, H.A., et al., 2018. Marine microbial metagenomes sampled across space and time. *Sci. Data* 5, 1–7.
- Bonin, P., Vieira, C., Grimaud, R., Militon, C., Cuny, P., Lima, O., Guasco, S., Brussaard, C.P.D., Michotey, V., 2015. Substrates specialization in lipid compounds and hydrocarbons of *Marinobacter* genus. *Environ. Sci. Pollut. Res.* 22, 15347–15359.
- Bowers, R.M., Kyrpides, N.C., Stepanauskas, R., Harmon-Smith, M., Doud, D., Reddy, T.B.K., Schulz, F., Jarett, J., Rivers, A.R., Eloe-Fadrosh, E.A., et al., 2017. Minimum information about a single amplified genome (MISAG) and a metagenome-assembled genome (MIMAG) of bacteria and archaea. *Nat. Biotechnol.* 35, 725–731.
- Campbell, M.A., Chain, P.S.G., Dang, H., El Sheikh, A.F., Norton, J.M., Ward, N.L., Ward, B.B., Klotz, M.G., 2011. *Nitrosococcus watsonii* sp. nov., a new species of marine obligate ammonia-oxidizing bacteria that is not omnipresent in the world's oceans: calls to validate the names "*Nitrosococcus halophilus*" and "*Nitrosomonas mobilis*". *FEMS Microbiol. Ecol.* 76, 39–48.
- Campeão, M.E., Reis, L., Leomil, L., de Oliveira, L., Otsuki, K., Gardinali, P., Pelz, O., Valle, R., Thompson, F.L., Thompson, C.C., 2017. The deep-sea microbial community from the amazonian basin associated with oil degradation. *Front. Microbiol.* 8, 1–13.
- Chaumeil, P.-A., Mussig, A.J., Hugenholtz, P., Parks, D.H., 2019. GTDB-Tk: a toolkit to classify genomes with the genome taxonomy database. *Bioinformatics* 36, 1925–1927.
- Corinaldesi, C., 2015. New perspectives in benthic deep-sea microbial ecology. *Front. Mar. Sci.* 2, 1–12.
- Danovaro, R., Company, J.B., Corinaldesi, C., D'Onghia, G., Galil, B., Gambi, C., Gooday, A.J., Lampadariou, N., Luna, G.M., Morigi, C., et al., 2010. Deep-sea biodiversity in the Mediterranean Sea: the known, the unknown, and the unknowable. *PLoS One* 5.

- Danovaro, R., Snelgrove, P.V.R., Tyler, P., 2014. Challenging the paradigms of deep-sea ecology. *Trends Ecol. Evol.* 29, 465–475.
- Dubinsky, E.A., Conrad, M.E., Chakraborty, R., Bill, M., Borglin, S.E., Hollibaugh, J.T., Mason, O.U., M. Picens, Y., Reid, F.C., Stringfellow, W.T., et al., 2013. Succession of hydrocarbon-degrading bacteria in the aftermath of the deepwater horizon oil spill in the gulf of Mexico. *Environ. Sci. Technol.* 47, 10860–10867.
- Eglinton, G., Hamilton, R.J., 1967. Leaf epicuticular waxes. *Science* 156, 1322–1335.
- Fadina, O.A., Venancio, I.M., Belem, A., Silveira, C.S., Bertagnolli D de, C., Silva-Filho, E.V., Albuquerque, A.L.S., 2019. Paleoclimatic controls on mercury deposition in northeast Brazil since the last interglacial. *Quat. Sci. Rev.* 221, 105869.
- Francini-Filho, R.B., Asp, N.E., Siegle, E., Hocevar, J., Lowyck, K., D'Avila, N., Vasconcelos, A.A., Baitelo, R., Rezende, C.E., Omachi, C.Y., et al., 2018. Perspectives on the Great Amazon Reef: extension, biodiversity, and threats. *Front. Mar. Sci.* 5, 1–5.
- Garrigues, P., Parlanti, E., Lapouyade, R., Bellocq, J., 1988. Distribution of methylperylene isomers in selected sediments. *Geochim. Cosmochim. Acta* 52, 901–907.
- Harrower, M., Brewer, C.A., 2003. ColorBrewer.org: an online tool for selecting colour schemes for maps. *Cartogr. J.* 40, 27–37.
- Hedges, J.I., Ertel, J.R., 1982. Characterization of lignin by gas capillary chromatography of cupric oxide oxidation products. *Anal. Chem.* 54, 174–178.
- Hedges, J.I., Keil, R.G., Benner, R., 1997. What happens to terrestrial organic matter in the ocean. *Geology*, 129013363 [https://doi.org/10.1016/S0146-6380\(97\)00066-1](https://doi.org/10.1016/S0146-6380(97)00066-1).
- Huang, J.M., Baker, B.J., Li, J.T., Wang, Y., 2019. New microbial lineages capable of carbon fixation and nutrient cycling in deepsea sediments of the northern South China Sea. *Appl. Environ. Microbiol.* 85.
- Jennerjahn, T.C., Ittekkot, V., Arz, H.W., Behling, H., Pätzold, J., Wefer, G., 2004. Asynchronous terrestrial and marine signals of climate change during Heinrich events. *Science* 306, 2236–2239.
- Kimes, N.E., Callaghan, A.V., Aktas, D.F., Smith, W.L., Sunner, J., Golding, B.T., Drozdowska, M., Hazen, T.C., Sufliata, J.M., Morris, P.J., 2013. Metagenomic analysis and metabolite profiling of deep-sea sediments from the Gulf of Mexico following the Deepwater Horizon oil spill. *Front. Microbiol.* 4.
- Kodzius, R., Gojbori, T., 2015. Marine metagenomics as a source for bioprospecting. *Mar. Genomics* 24, 21–30.
- Kucera, M., 2007. Chapter six planktonic foraminifera as tracers of past oceanic environments. *Dev. Mar. Geol.* 1, 213–262.
- Lea-Smith, D.J., Biller, S.J., Davey, M.P., Cotton, C.A.R., Sepulveda, B.M.P., Turchyn, A.V., Scanlan, D.J., Smith, A.G., Chisholm, S.W., Howe, C.J., 2015. Contribution of cyanobacterial alkane production to the ocean hydrocarbon cycle. *Proc. Natl. Acad. Sci. U. S. A.* 112, 13591–13596.
- Lim, S., Chang, D.H., Kim, B.C., 2016. Whole-genome sequence of *Sunxiuqinia dokdonensis* DH1T, isolated from deep sub-seafloor sediment in Dokdo Island. *Genomics Data* 9, 95–96.
- Meyer, F., Bagchi, S., Chaterji, S., Gerlach, W., Grama, A., Harrison, T., Paczian, T., Trimble, W.L., Wilke, A., 2018. MG-RAST version 4: lessons learned from a decade of low-budget ultra-high-throughput metagenome analysis. *Brief. Bioinform.* 20, 1151–1159.
- Moura, R.L., Amado-Filho, G.M., Moraes, F.C., Brasileiro, P.S., Salomon, P.S., Mahiques, M.M., Bastos, A.C., Almeida, M.G., Silva, J.M., Araujo, B.F., et al., 2016. An extensive reef system at the Amazon River mouth. *Sci. Adv.* 2, 1–12.
- Mullineaux, L.S., Metaxas, A., Beaulieu, S.E., Bright, M., Gollner, S., Grupe, B.M., Herrera, S., Kellner, J.B., Levin, L.A., Mitarai, S., et al., 2018. Exploring the ecology of deep-sea hydrothermal vents in a metacommunity framework. *Front. Mar. Sci.* 4.
- Naether, D.J., Slawtschew, S., Stasik, S., Engel, M., Olzog, M., Wick, L.Y., Timmis, K.N., Heipieper, H.J., 2013. Adaptation of the hydrocarbonoclastic bacterium *Alcanivorax borkumensis* SK2 to alkanes and toxic organic compounds: a physiological and transcriptomic approach. *Appl. Environ. Microbiol.* 79, 4282–4293.
- Nurk, S., Meleshko, D., Korobeynikov, A., Pevzner, P.A., 2017. MetaSPAdes: a new versatile metagenomic assembler. *Genome Res.* 27, 824–834.
- Orsi, W.D., Coolen, M.J.L., Wuchter, C., He, L., More, K.D., Irigoien, X., Chust, G., Johnson, C., Hemingway, J.D., Lee, M., et al., 2017. Climate oscillations reflected within the microbiome of Arabian Sea sediments. *Sci. Rep.* 7, 1–12.
- Paradis, E., Claude, J., Strimmer, K., 2004. APE: analyses of phylogenetics and evolution in R language. *Bioinformatics* 20, 289–290.
- Parks, D.H., Imelfort, M., Skennerton, C.T., Hugenholtz, P., Tyson, G.W., 2015. CheckM: assessing the quality of microbial genomes recovered from isolates, single cells, and metagenomes. *Genome Res.* 25, 1043–1055.
- Parks, D.H., Chuvochina, M., Waite, D.W., Rinke, C., Skarshewski, A., Chaumeil, P.A., Hugenholtz, P., 2018. A standardized bacterial taxonomy based on genome phylogeny substantially revises the tree of life. *Nat. Biotechnol.* 36, 996.
- Parks, D.H., Chuvochina, M., Chaumeil, P., et al., 2020. A complete domain-to-species taxonomy for Bacteria and Archaea. *Nat. Biotechnol.* <https://doi.org/10.1038/s41587-020-0501-8>.
- R Core Team, 2019. R: a language and Environment for statistical computing. Available from: <https://www.r-project.org>.
- Rühlemann, C., Frank, M., Hale, W., Mangini, A., Mulitza, S., Müller, P., Wefer, G., 1996. Late quaternary productivity changes in the western equatorial Atlantic: evidence from 230Th-normalized carbonate and organic carbon accumulation rates. *Mar. Geol.* 135, 127–152.
- Schmieder, R., Edwards, R., 2011. Quality control and preprocessing of metagenomic datasets. *Bioinformatics* 27, 863–864.
- Shin, S., Kahng, H.Y., 2017. *Cyclobacterium sediminis* sp. nov. isolated from a sea cucumber aquaculture farm and emended description of the genus *Cyclobacterium*. *J. Microbiol.* 55, 90–95.
- Silliman, J.E., Meyers, P.A., Eadie, B.J., 1998. Perylene: an indicator of alteration processes or precursor materials? *Org. Geochem.* 29, 1737–1744.
- Simoneit, B., Chester, R., Eglinton, G., 1977. Biogenic lipids in particulates from the lower atmosphere over the eastern Atlantic. *Nature* 267, 682–685.
- Tesi, T., Miserocchi, S., Goñi, M.A., Langone, L., Boldrin, A., Turchetto, M., 2007. Organic matter origin and distribution in suspended particulate materials and surficial sediments from the western Adriatic Sea (Italy). *Estuar. Coast. Shelf Sci.* 73, 431–446.
- Throne-Holst, M., Wentzel, A., Ellingsen, T.E., Kotlar, H.K., Zotchev, S.B., 2007. Identification of novel genes involved in long-chain n-alkane degradation by *Acinetobacter* sp. strain DSM 17874. *Appl. Environ. Microbiol.* 73, 3327–3332.
- U.S. Environmental Protection Agency, 1996. SW-846 test method 3540C: Soxhlet extraction, part of test methods for evaluating solid waste. 3rd Edition. Physical/Chemical Methods 4 pp. 1–8.
- U.S. Environmental Protection Agency, 2014. SW-846 Method 8270E: Semivolatile Organic Compounds by Gas Chromatography/Mass Spectrometry (GC-MS) (64pp).
- Venancio, I.M., Mulitza, S., Govin, A., Santos, T.P., Lessa, D.O., Albuquerque, A.L.S., Chiessi, C.M., Tiedemann, R., Vahlenkamp, M., Bickert, T., et al., 2018. Millennial- to orbital-scale responses of Western equatorial Atlantic thermocline depth to changes in the trade wind system since the last interglacial. *Paleoceanogr. Paleoclimatology* 33, 1490–1507.
- Vuillemin, A., Wankel, S.D., Coskun, Ö.K., Magritsch, T., Vargas, S., Estes, E.R., Spivack, A.J., Smith, D.C., Pockalny, R., Murray, R.W., et al., 2019. Archaea dominate oxic subseafloor communities over multimillion-year time scales. *Sci. Adv.* 5, 1–12.
- Wakeham, S.G., Canuel, E.A., 1988. Organic geochemistry of particulate matter in the eastern tropical North Pacific Ocean: implications for particle dynamics. *J. Mar. Res.* 46, 183–213.
- Wang, W., Shao, Z., 2013. Enzymes and genes involved in aerobic alkane degradation. *Front. Microbiol.* 4, 1–7.
- Wickham, H., 2007. Reshaping data with the reshape package. *J. Stat. Softw.* 21, 1–20.
- Wickham, H., Averick, M., Bryan, J., Chang, W., McGowan, L., François, R., Grolemund, G., Hayes, A., Henry, L., Hester, J., et al., 2019. Welcome to the Tidyverse. *J. Open Source Softw.* 4, 1686.
- Wolff, E.W., Chappellaz, J., Blunier, T., Rasmussen, S.O., Svensson, A., 2010. Millennial-scale variability during the last glacial: the ice core record. *Quat. Sci. Rev.* 29, 2828–2838.
- Yakimov, M., Golyshin, P., Crisafi, F., Denaro, R., Giuliano, L., 2019. Marine, aerobic hydrocarbon-degrading Gammaproteobacteria: the family Alcanivoraceae. In: McGenety, T. (Ed.), *Taxonomy, Genomics and Ecophysiology of Hydrocarbon-Degrading Microbes*. Handbook of Hydrocarbon and Lipid Microbiology. Springer, Cham, p. 382.
- Zadjeleovic, V., Chhun, A., Quareshy, M., Silvano, E., Hernandez-Fernaund, J.R., Aguilo-Ferretjans, M.M., Bosch, R., Dorador, C., Gibson, M.I., Christie-Oleza, J.A., 2020a. Beyond oil degradation: enzymatic potential of Alcanivorax to degrade natural and synthetic polyesters. *Environ. Microbiol.* 22, 1356–1369.
- Zadjeleovic, V., Gibson, M.I., Dorador, C., Christie-Oleza, J.A., 2020b. Genome of Alcanivorax sp. 24: a hydrocarbon degrading bacterium isolated from marine plastic debris. *Mar. Genomics* 49, 100686.
- Zhang, J., Kobert, K., Flouri, T., Stamatakis, A., 2014. PEAR: a fast and accurate Illumina paired-end reAd merger. *Bioinformatics* 30, 614–620.